Project Description

1 Rationale and Objectives

Manipulation of the nitrogen—vacancy (NV) center charge state provides many opportunities for advancing the progress of quantum sensing technologies and the fundamental understanding of key aspects of the NV system.

Manipulation of the NV charge-state can be used to explore fundamental properties of the NV itself. There is still much debate about the magnitude and temperature dependence of the energy gap between the metastable singlet state and other features within the band structure of the NV center [1–23], which could be resolved by employing photoionization of the metastable singlet state in order to determine the single-photon ionization resonance wavelength of the singlet state. This measurement can be repeated for many temperatures, thereby providing insight into the temperature dependence of the singlet-triplet energy gap.

As a part of the proposed research, we plan to investigate the separation of the singlet state of the NV^- from the conduction band edge by employing a wavelength- dependent photoionization regime involving pulsed microwave excitation, laser charge- state initialization and readout pulses, and ultrashort laser pulses for wavelength- tunable photoionization. NV diamond (NVD) samples will have interdigital metal electrodes written onto their surfaces using a direct write lithography technique that will provide an average electrode separation of 10 μm. These electrodes will facilitate measurement of photocurrent generated by incident laser radiation. The charge distribution of NV centers between the sample electrodes will be initialized into a majority NV^- configuration using an intense pulse of green laser radiation, followed by selective population of the NV- singlet state and initial charge- state readout via a sequential microwave and charge-state readout pulse, whereupon a pulse of wavelength-tunable laser radiation will be applied to the NV for attempted photoionization into the neutrally charged NV center (NV^0), while photocurrent from the diamond is read out to detect the effects of the photoionization pulse. A final laser charge-state readout pulse will be applied in order to detect the change in charge distribution after the ionization pulse. This spin-selective photoionization pulse regime ties the fluorescence excited from the subsequent NV charge distribution to the photocurrent from the sample as a function of ionization wavelength while the NV centers are deterministically within the singlet state, thereby determining the wavelength of the singlet state single photon ionization resonance. In a subsequent section of the proposed research, we plan to place these NVD samples into a thermally controlled chamber and measure the singlet state single photon ionization resonance using the methods described above as a function of the temperature of the sample. Finally, we plan to incorporate these samples onto the tip of optical fiber quantum sensing probe, and characterize the improvement in the magnetic resonance contrast and quantum sensing capabilities of this probe when using a dual-beam photoelectric detected magnetic resonance (PDMR) measurement protocol compared to our previous generation of fiber-optic probes that employed only optically detected magnetic resonance (ODMR).

The proposed research program includes three work packages. In the first work package, we plan to fabricate NVD samples containing printed metal electrodes for photocurrent detectionas, and as a proof of principle we propose to demonstrate the ability of our correlated single-shot charge state and photoelectric detection ionization regime to measure the singlet-triplet energy gap of the NV center singlet state . The second work package will involve inserting the NV samples fabricated in the first work package into a temperature controlled liquid helium cryostat and measuring the effect of thermal fluctuations on the singlet-triplet energy gap. The third work package will involve the fabrication of a PDMR capable fiber-optic probe and a proof of principle demonstration of

improved magnetic resonance contrast and subsequently improved quantum sensing capabilities of this device compared to previous fiber quantum sensor technology employing ODMR.

2 State of the Art and Motivation

Manipulation of the NV center charge state has proven to be to be an effective tool for both super-resolution microscopy and spectroscopy.

Manipulation of the NV center charge state has already opened the door for unique ways to perform spectroscopy on the NV center itself. Recent experimental measurements and theoretical calculations performed at cryogenic temperatures have demonstrated an energy gap on the order of 300 meV between the 1E and the $^3A_2$ state, while theoretical calculations combined with experimental data taken at temperatures above 300 K have determined the two levels to be almost degenerate in energy. This discrepancy, when viewed in light of the relative temperature independence of the infrared $^1A \rightarrow {}^1E$ singlet transition, suggests a temperature dependence of the relative location of the $^1A/^1E$ singlet level pair with respect to the $^3A_2$ state.

Photoionization of the NV center has also been used to perform high contrast magnetic resonance measurements by reading out the change in fluorescence intensity as the defect ionizes and also by measuring the changes in photocurrent emitted by the sample in the presence of ionizing laser excitation. These magnetic resonance techniques have also been used to detect weak magnetic field fluctuations in the vicinity of the vacancy sites.

Fiber-optic NVD probes represent the bleeding edge of technological innovation when it comes to satisfying the need for minimally invasive quantum sensing of temperature or magnetic field in an in vivo environment. However, these probes suffer from a lack of ODMR contrast as a result of their inability to out-of-focus signal from the diamond.

The combination of PDMR and fiber-optic NVD probes can concievably enhance the contrast of these quantum probes, pushing this technology into new and interesting sensing paradigms.

3 Methodology and General Work Program

The principle aspect of the NV system that enables its quantum sensing capabilities is its optically accessible triplet state transition that possesses spin-dependent fluorescence amplitude. The electron spin of individual center can be manipulated by light, magnetic, electric and microwave fields, enabling high precision measurements of electromagnetic fields and temperature distributions. Optical initialization of the NV- can be achieved with wavelengths between 480 nm and 637 nm, with the most common techniques using a 532 nm source based on second-harmonic output of a Nd:YAG laser. This laser radiation couples the $^3A_2$ ground electronic state to the ^3E excited state, giving rise to photoluminescence (downward red arrows, Fig.1b, right), featuring a characteristic zero-phonon line, which is observed at approximately 637 nm at room temperature against a broad phonon-sideband stretching into the NIR (Fig. 1a, left). The electron spin of the NV ground-state triplet can be manipulated by a microwave field via electron spin resonance (ESR). The spin part of the electron Hamiltonian of an NV center in the presence of an external magnetic field B is written as $H_s = \mu_b g \mathbf{B} \cdot \mathbf{s} + hD[S_z^2 - \frac{S(S+1)}{3}] + hE(S_x^2 - S_y^2)$, where μ_b is the Bohr magneton, $g \approx 2$ is the electron g-ratio, D and E are the zero magnetic field splitting parameters, and S_j $(j = x, y, z)$ are the projections of the electron spin $\mathbf{S}$ on the principal Cartesian coordinate axes x, y, z, with the z-axis chosen along the NV axis. The first term in this Hamiltonian describes the Zeeman effect in an external magnetic field, which is observed against zero-field splitting due to spin-spin interactions in the vacancy site. This zero field splitting is governed by the second and third terms in H_s, dominated by the splitting $\Omega_s = D \approx 2.87$GHz (where h is the Planck constant) between

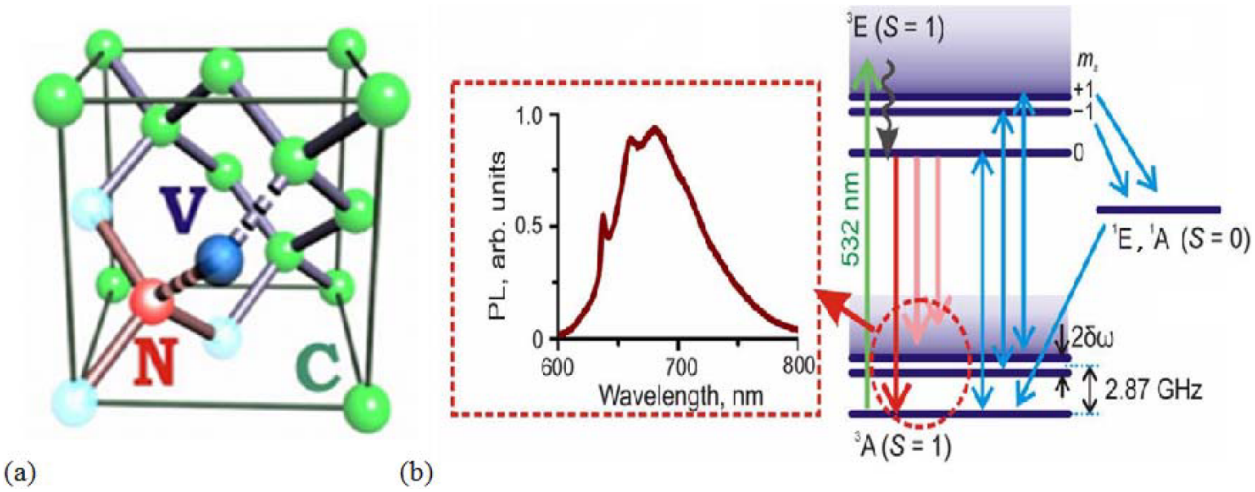

Figure 1: (a) A nitrogen atom (N) and a vacancy (V) forming an NV center in a diamond lattice, consisting of carbon (C) atoms. Four possible arrangements of the NV axis with respect to the crystal lattice of diamond are shown. (b) Diagram of energy levels involved in electron-spin spectroscopy. The ground state of NV- is a spin-triplet state with a zero-field splitting $\Omega_s \approx 2.87GHz$. When tuned to the ESR frequency Ω_s, a microwave field efficiently transfers population from the $m_s = 0$ to the $m_s = \pm 1$ state. An optical pump at 532nm couples the $^3A_2$ ground electronic state to the ^{3}E excited state, giving rise to photoluminescence, shown by the red line, featuring a characteristic zero-phonon line at approximately 637 nm, which is observed in the spectrum of photoluminescence (shown on the left) against a broad phonon-sideband line, stretching down to 800 nm. An external magnetic field removes the degeneracy of the $m_s = \pm 1$ state and induces a Zeeman frequency shift $2\delta\omega$ between these sublevels. A substantial fraction of the $m_s = \pm 1$ excited-state population is transferred to the $m_s = 0$ ground level via a metastable ^1E singlet state.

the $m_s = 0$ spin state and the twofold-degenerate $m_s = \pm 1$ state (Fig. 1b). When the microwave field is tuned to the ESR frequency Ω_s, this microwave field efficiently transfers population from the $m_s = 0$ to the $m_s = \pm 1$ state (Fig. 1b), thus manipulating spin orientation. For an NV^- in the $m_s = \pm 1$ state, the photoluminescence yield is lower than that typical of NV^- in the $m_s = 0$ state. This is because a substantial fraction of the $m_s = \pm 1$ excited state population is non-radiatively transferred to the $m_s = 0$ ground level via a metastable singlet state (^{1}E state in Fig. 1b). This pathway allows for optical readout of the spin state by analyzing the intensity of the photoluminescence signal. An external magnetic field B removes the degeneracy of the $m_s = \pm 1$ state and induces a Zeeman frequency splitting $\Delta\Omega_Z$ between the $m_s = \pm 1$ sublevels (Fig. 1b). Since the photoluminescence from $m_s = \pm 1$ levels is weaker than the photoluminescence from $m_s = 0$ states, the Zeeman-shifted sublevels are observed as B- dependent features in the ODMR spectrum measured as a function of the microwave frequency Ω. The ODMR spectrum changes as a function of applied magnetic field and as a function of NVD temperature. As the magnetic field increases, the projection of the magnetic field onto the four quantization axes present in a bulk NVD will induce shifts in the corresponding eight ODMR peaks present (one for each spin sublevel in each of four quantization axes), causing the peaks to spread apart (Fig. 2a). Temperature manifests as strain in the NVD lattice, and the effect of this strain is to shift the zero-field splitting (parameter D) by -75 kHz/K (Fig. 2b).

The NV^0 charge state can also be used to assist in the quantum sensing applications of the

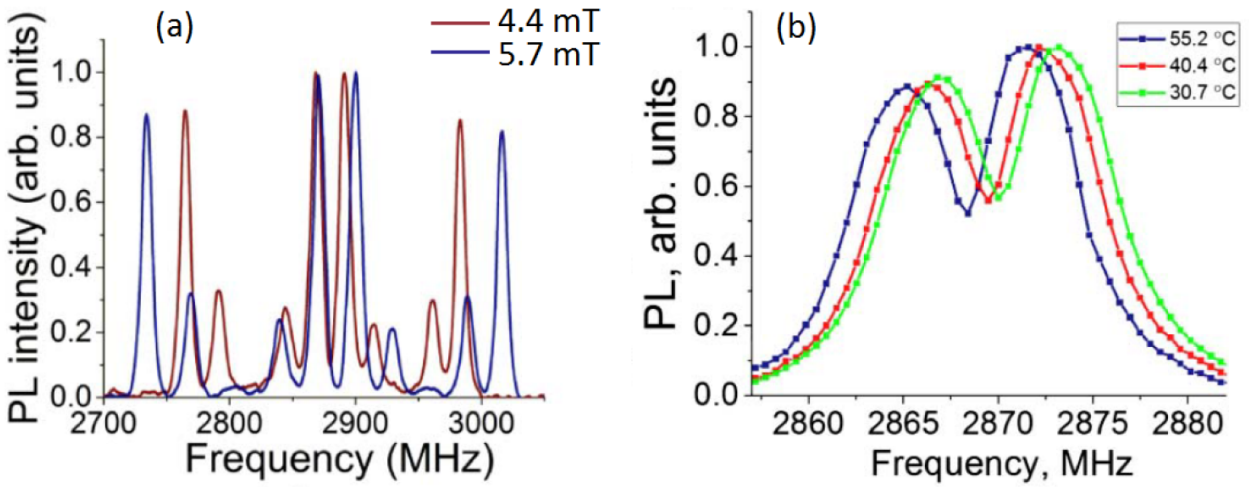

Figure 2: Previous ODMR measurements. (a) Shown is the spreading of the 8 ODMR peaks due to an external magnetic field. (b) Plot showing the shift of the ODMR peaks due to a change in external temperature. This shift was measured to be -75 kHz/K.

NV center, and is accessible from the NV^- by photoionization of the electron occupying the triplet state in the vacancy site via either a resonant single-photon ionization process with wavelength < 476 nm (Fig. 3, blue arrows) or via a two-photon ionization process with wavelength < 637 nm that uses the excited state as an intermediate transition. The NV^0 charge state itself possesses a broad fluorescent transition with a zero-phonon line (ZPL) at 575 nm. Once the NV^- is ionized, it is possible to convert the NV^0 back into an NV^- by a two-photon recombination regime (Fig. 3, green arrows on right). The NV^0 is excited into the $^2A_1$ excited state with 532 nm radiation which also pulls an electron from the valence band into the ^2E ground state, converting the NV^0 back into an NV^-. At 637 nm excitation wavelengths, the ionization rate of the NV^- is at least one order of magnitude larger than the recombination rate of the NV^0, making it possible to transfer above 90% of the NV center population of an NVD within the focal region of the excitation into the NV^0 charge state. Because NV centers cannot be excited by wavelengths greater than the wavelength of their ZPL, it is possible to selectively stimulate only the NV^- centers in a diamond with laser wavelengths between the 575 nm NV^0 ZPL and the 637 nm NV^- ZPL.

The proposed research is aimed at advancing the fundamental understanding of the NV singlet state that will inspire new and novel high contrast optical, temperature, and magnetic field imaging techniques.

Correspondingly, the proposed activities are divided into the following work packages (WP): Photoionization assisted singlet-state spectroscopy (WP1), spectroscopic investigations of the effect of temperature on the NV^- singlet-triplet energy gap (WP2), and design, fabrication, and testing of a PDMR based fiber-optic sensor (WP3). Wherein the samples fabricated in WP1 will be used in each subsequent work plan.

3.1 WP1: Photoionization Assisted Spectroscopy of the NV^- Singlet State

As a part of the proposed research, we plan to investigate the separation of the NV singlet state from the triplet ground state by employing a wavelength-dependent photoionization regime involving pulsed microwave radiation, wavelength-tunable laser excitation, and pulsed bichromatic initialization and readout laser excitation. The singlet states of NV centers in a high NV concentra-

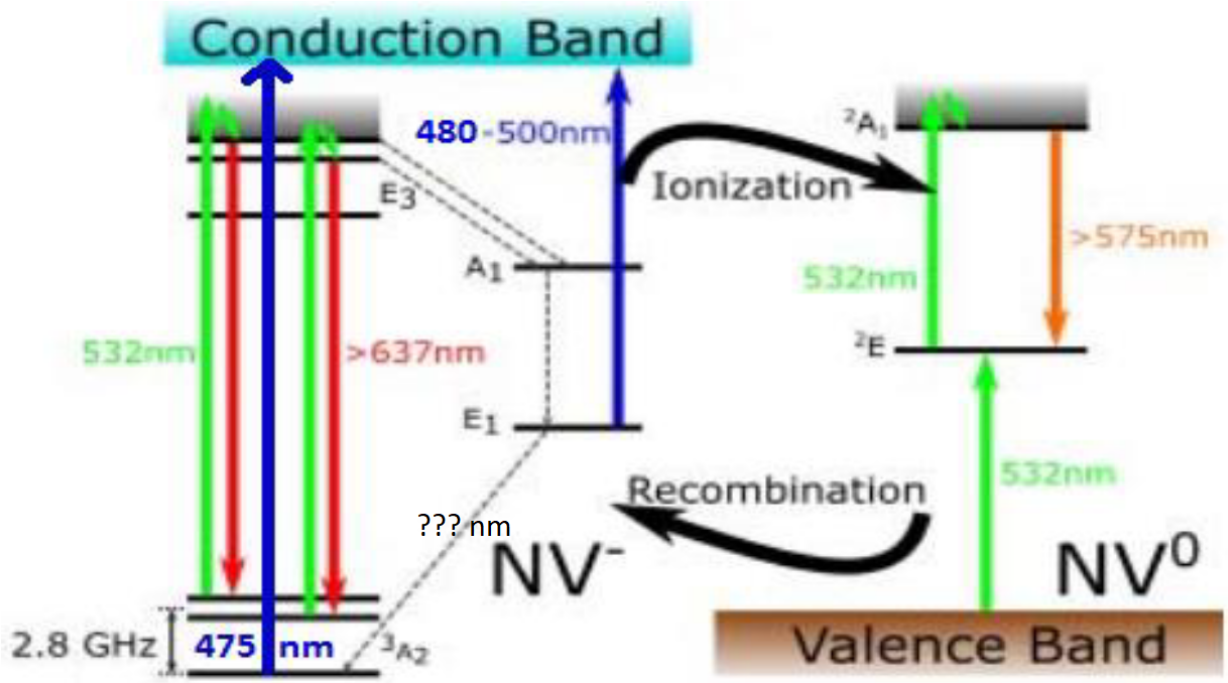

Figure 3: Level diagram of the NV and NV^0 states and their relative separation from the conduction and valence band edges. Blue arrows represent wavelengths required for single-photon ionization from the ground state and from the excited state. Green arrows represent wavelengths used to excite the defects into their excited states, or to induce recombination from NV^0 to NV^-. Orange and red arrows represent fluorescence wavelengths of the zero phonon line from resulting excitation with 532 nm light.

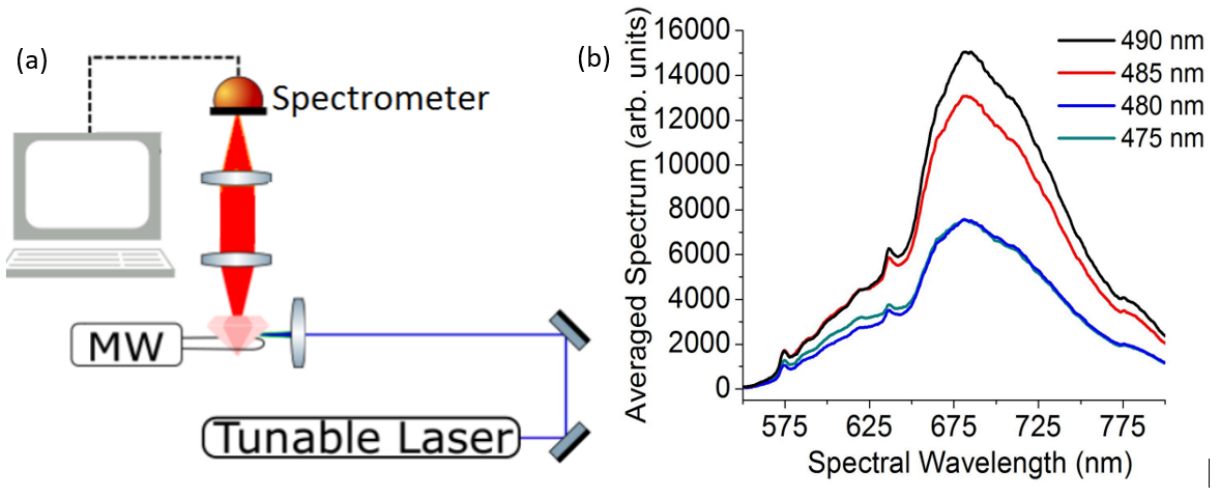

Figure 4: (a) Diagram of the experimental setup for preliminary photoionization measurements. (b) Fluorescence spectra of the NV sample taken with multiple excitation wavelengths.

tion diamond sample will be populated through a spin-selective intersystem crossing (ISC) with a sequential laser initialization and microwave pulse train, whereupon a pulse of wavelength-tunable laser radiation will be applied to the sample. When the wavelength-tunable laser radiation is in resonance with the energy gap between the recently populated metastable singlet state and the conduction band of the diamond sample, a fraction of the NV centers will be ionized into neutrally charged NV centers (NV^0). Given that the NV^0 zero- phonon line occurs at 575 nm, laser excitation with wavelengths longer than 575 nm cannot excite the NV^0.

Previous measurements attempting to demonstrate singlet state photoionization were performed using the wavelength tunable output of a supercontinuum laser and simultaneous resonant microwave excitation (Fig. 4(a)). The fluorescent output of the NV sample was coupled into a spectrometer, and multiple spectra were recorded for a range of excitation wavelengths between 475 and 490 nm (Fig. 4(b)).

Each of these spectra were recorded in the presence of and in the absence of resonant microwave excitation. The ratio of these spectra were calculated, and ratios of fluorescence amplitudes corresponding to regions of the spectra belonging to the NV^0 were compared to those of the NV^- centers. In the presence of a resonant microwave field, when the laser wavelengths are tuned to the single photon ionization resonance between the metastable singlet state and the conduction band, the fluorescence in the NV^0 region of the spectrum is expected to increase with respect to the fluorescence in the NV^- region. This is because the when the laser excitation is at the singlet state single photon ionization resonance, a fraction of the singlet state population is ionized into the neutrally charged state, thereby providing a relative increase in fluorescence in the NV^0 region of the spectrum in the presence of microwave excitation, and a corresponding relative decrease in NV fluorescence (Fig. 5(a)). The spectral ratios taken in this experiment indicate an ionization resonance around 480 nm, manifesting as the largest NV^0/NV^- fluorescence ratio at that ionization wavelength (Fig. 5(b)), which agrees with the single photon ionization resonance described in the literature.

Applying red pulses (λ ¿ 575 nm) before and after the ionization pulse provides a convenient way to read out the ionization induced relative NV population difference induced by the ionization pulse. Because these red pulses cannot excite the NV^0 centers, any ionization induced population

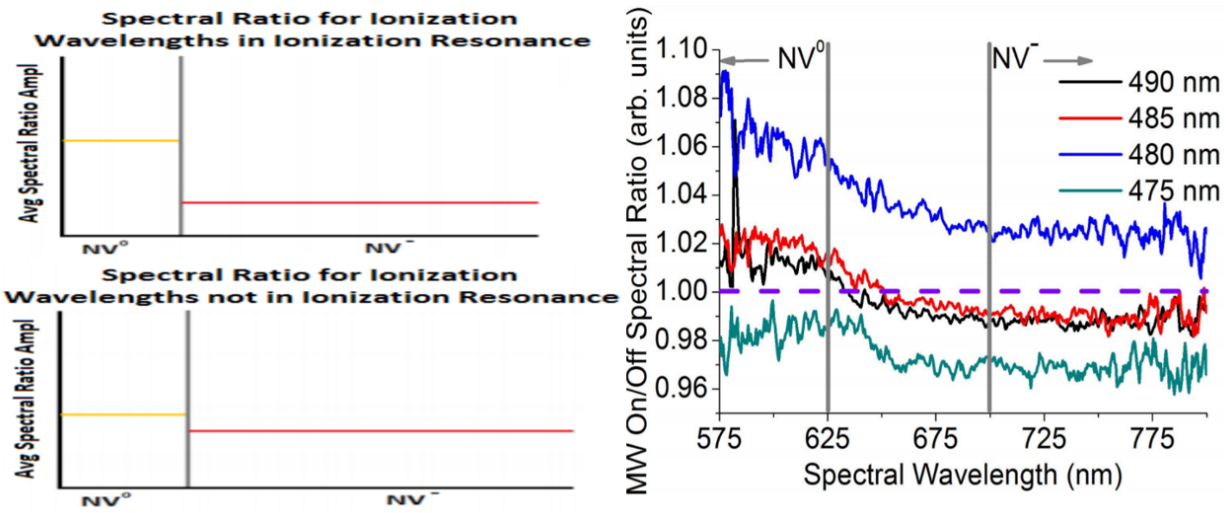

Figure 5: (a) expected behavior of fluorescence ratio between spectral measurements with microwave field on/off at ionization resonance and away from ionization resonance. (b) Experimental results taken with 50 mW of excitation power in high-concentration NV sample demonstrating predicted behavior.

changes will be apparent by analyzing the change in fluorescence intensity recorded between the two pulses. Attaching electrodes to the diamond and measuring the photocurrent induced by the ionization pulse will provide confirmation of photoionization at resonant wavelengths. By varying the wavelength of the ionization pulse, it will be possible to determine the single-photon ionization resonance energy for the NV singlet state at a given temperature. Using an optically detected magnetic resonance technique, it is possible to determine the temperature of the diamond sample prior to each photoionization measurement. By placing the sample in a thermally stabilized environment with controllable temperature, it will be possible to produce a plot of the dependence of the singlet-triplet energy gap on temperature.

Our experimental plan to demonstrate NV singlet ionization in this work package will involve a pulse train system created by using acousto-optic modulators (AOMs) to modulate incident radiation from a 532 nm Nd:YAG laser source, a 637 nm diode laser source, and a picosecond supercontinuum source and synchronizing these pulses with pi pulses from a microwave oscillator (Fig. 6). This pulse regime will involve pumping the NV center into the singlet state by first spin polarizing the NV center into the $m_s = 0$ ground state sublevel with a pulse of 532nm laser excitation lasting approximately 1 μs (Fig. 6, green trace). This pulse also serves to redistribute the charge states of the NV/NV^0 present in the sample into an equilibrium distribution via two-photon ionization/recombination. A microwave pi pulse tuned to the frequency of either $m_s = \pm 1$ ground state sublevels (Fig. 6, brown trace) followed immediately by a 100 ns 637 nm pulse will populate the metastable singlet state (Fig. 6, red trace). The function of the red laser pulse is twofold. It serves as a mechanism for populating the singlet state by exciting the population in the ground state to the excited state, whereupon an ISC carries the population into the metastable singlet state. It also serves as an initial readout of the charge distribution of the sample by selectively exciting the NV population without stimulating the NV^0 population. A wavelength tunable picosecond pulse from a supercontinuum laser will either ionize or fail to ionize the NV center (Fig. 6, blue trace), at which point a second 637 nm pulse identical to the first will arrive within one lifetime of the metastable singlet state of the previous red pulse and readout the relative change in charge

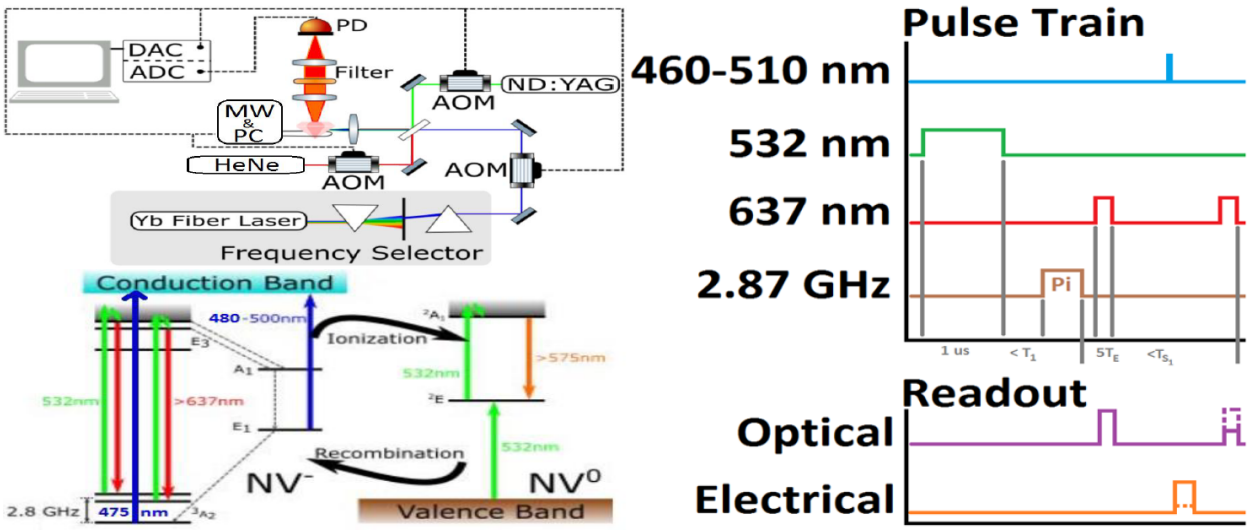

Figure 6: (a) Experimental diagram of the system for ionizing the NV singlet state. All fluorescence signal collected by photodiode (PD) through a 700 nm long pass filter. Photocurrent (PC) signals collected using picoammeter. All signal outputs analyzed with 14 bit analog to digital converter. (b) Proposed pulse train.

distribution of the sample. The relative change in readout between the first and second red pulses (Fig. 6, purple trace) as a function of ionization wavelength, in conjunction with the correlated photocurrent measurements taken at the time of arrival of the ionization pulse (Fig. 6, orange trace) will provide the separation of the singlet state from the conduction band edge at that temperature.

3.2 WP2: Spectroscopic Investigations of the Effect of Temperature on the NV^- Singlet-Triplet Energy Gap

In this work project, we propose to investigate the as of yet unexplored temperature dependence of the singlet-triplet energy gap in the NV^- center. The temperature of the sample will be measured before each ionization measurement using the optically detected magnetic resonance technique . These temperature measurements will be optimized in sensitivity by plotting the maximum slope of the ODMR peaks as a function of input microwave power and laser power (Fig. 7(a)), providing the necessary parameters for optimal sensitivity of the temperature measurement. The sample's sensitivity to temperature fluctuations are recorded using the noise trace technique described in (Fig. 7(b)).

Temperature sensitivity below that of the minimum temperature control increment that the system is capable of is desirable. Once this sensitivity has been verified, ionization measurements described in WP3 can be performed at small temperature increments between 4K and 300K, and the dependence of the triplet-singlet energy gap on temperature can be plotted.

In order to facilitate accurate temperature measurements over a broad range of temperatures, a liquid helium cryostat with built in confocal microscope will be used in order to thermally stabilize and control the system (Fig. 9). This cryostat contains a heating element capable of accurately manipulating the temperature of the sample environment in single Kelvin increments.

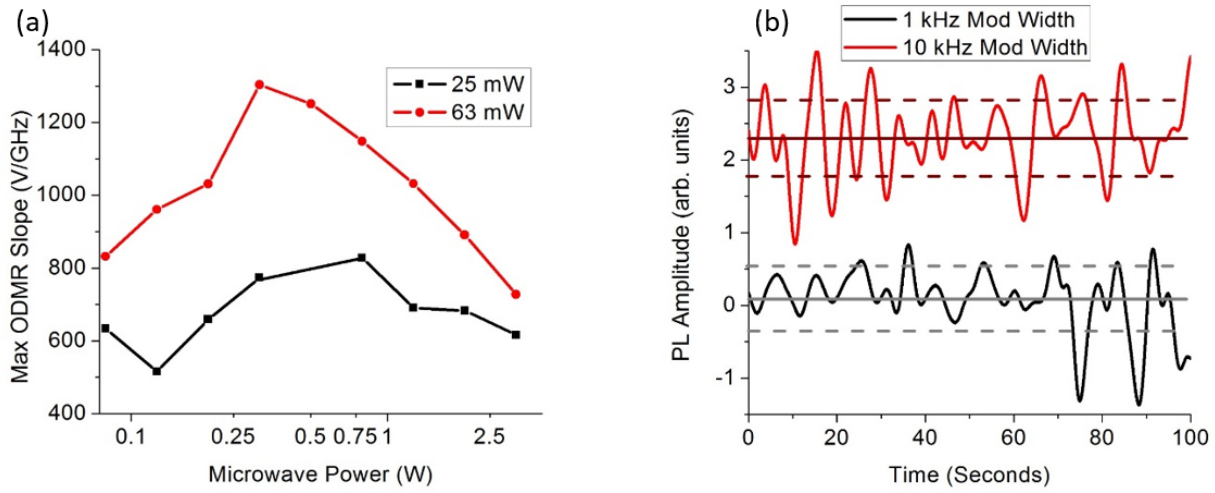

Figure 7: (a) Maximum ODMR slope measured at multiple microwave power levels and two laser power levels for high NV density sample. (b) Noise traces depicting a temperature sensitivity of 125 mK/$\sqrt{\text{Hz}}$ for the sample within the thermally stabilized chamber.

3.3 WP3: Enhanced Fiber-Optic Quantum Sensing with Photoelectric Detected Magnetic Resonance

In this work project we propose to improve upon existing fiber-optic quantum probe technology by incorporating the samples fabricated in WP1 and utilizing a PDMR regime to enhance the magnetic resonance contrast in a fiber-optic probe with integrated NVD.

4 Mechanisms to Assess Success

The success of the research under each work package will be assessed by the following criteria:

- The success of the work under WP1 will be judged by successfully attaching electrodes to the diamond samples and a successfull proof of principle demonstration of ionization of the NV center singlet state whereby we will measure both the differential fluorescence output from between the two charge-state readout pulses and the change in photocurrent collected during the ionization pulse to characterize the N_s^0/NV ratio of the sample in order to distinguish the NV center contributions to the photocurrent from that of the N_s^0 defect. Another goal of WP1 will be to then identify the peak in detected NV center photocurrent at the location of the singlet level ionization resonance with the conduction band as a function of input ionization wavelength, and to corroborate this measurement by observing a differential fluorescence signal between the two charge-state readout pulses that corresponds to the number of ionized NV centers measured using the photocurrent method.

- The success of the work under WP2 will be judged successfully using the samples produced and tested in WP1 to generate a plot of the singlet-triplet energy gap as a function of temperature.

- The success of the work under WP3 will be judged by a proof of principle measurement of the photocurrent signal originating from the NV centers within an NV sample located at the tip of a fiber-optic PDMR probe, and a subsequent full characterization of the relative enhancement of magnetic resonance contrast and magnetic field/temperature sensitivity of

the PDMR fiber probe compared to previous ODMR based fiber probe devices developed in this lab.

5 Intellectual Merit

The proposed experimental plan will resolve important open questions about the singlet state energy level structure by exploring the previously unknown temperature dependence of the energy difference between the ground state triplet and the metastable singlet energy levels in the NV center, as well as will create compact fiber-optic PDMR quantum sensors with leading-edge sensitivity and lower laser power profiles for use in sensitive biological environments.

6 Broader Impact

Research on the use of charge state manipulation for spectroscopy and for improved fiber-optic quantum sensors will be disseminated at conferences, in publications, patent applications, and research materials for undergraduate and graduate students. Furthermore, the proposed research will provide worthwhile opportunities for women, educationally underserved populations, and children in grades K-12 interested in Science, Technology, Engineering, and Mathematics (STEM) subjects through various outreach activities.

6.1 Efforts in International Science Communication

The PI Dr. Aleksei Zheltikov has regularly been a guest on numerous television programs in multiple countries promoting the benefits of science education to an international audience. Dr. Zheltikov involves his team of graduate and undergraduate students in the planning, production, and design of the program for these presentations, and presents their recent work to an audience of all ages in an accessable way.

6.2 Educational Outreach Program - The Physics and Engineering Festival

It is proposed to contribute multiple hands on demonstrations to the annual Texas A&M Physics and Engineering festival. The Texas A&M Physics and Engineering festival is an annual tradition at Texas A&M Univeristy aimed at generating enthusiasm and participation in STEM subjects in people of all ages by providing a day of hands on science experimental demonstrations lectures by distinguished scientists. We will present STEM demonstrations in the area of basic fiber-optics (total internal reflection in a stream of water) to illustrate how fiber-optics are integrated into existing technology (image transmission with fiber bundles), and how they can be a critical component of newer technologies (fiber optic magnetic field sensors). These optics demonstrations will be led by PhD students Joe Becker and Yusef Maleki, as well as post-doctoral researcher Sean Blakley.

6.3 International Exchange Program

An educational outreach program is proposed to develop closer ties with international collaborators and to coordinate work on problems of mutual interest. It is proposed to create expand the existing research partnership between the PI's group at Texas A&M University and his groups at the Russian Quantum Center in Skolkovo, Russia and at Moscow State University in Moscow, Russia, via a student exchange program, as well as to foster a student exchange relationship with allied groups at the Technical University of Vienna.

7 Results from Prior NSF Support

Not Applicable.